

Supporting Information

Enabling Multidimensional Fine-Tuning of Large Scale BiOI Films with Ultrasonic Spray Pyrolysis

Hao Wang^{a,b}, *Weilong Qin*^b, *Qitao Liu*^b, *Neway Belachew*^b, *Jianming Li*^c, *Qinglu Liu*^d,

Jiabo Le^b, *Yongbo Kuang*^{b,*}

a School of Materials Science and Chemical Engineering, Ningbo University, Ningbo, Zhejiang 315211, China

b Zhejiang Key Laboratory of Advanced Fuel Cells and Electrolyzes Technology, Ningbo Institute of Materials Technology and Engineering, Chinese Academy of Sciences, Ningbo, Zhejiang, 315201, China

c Institute of Materials, Ningbo University of Technology, Ningbo 315211, China

d Center of Artificial Photosynthesis for Solar Fuels and Department of Chemistry, School of Science and Research Center for Industries of the Future, Westlake University, Hangzhou, Zhejiang 310030, China

*Corresponding Author

Correspondence: kuangyongbo@nimte.ac.cn

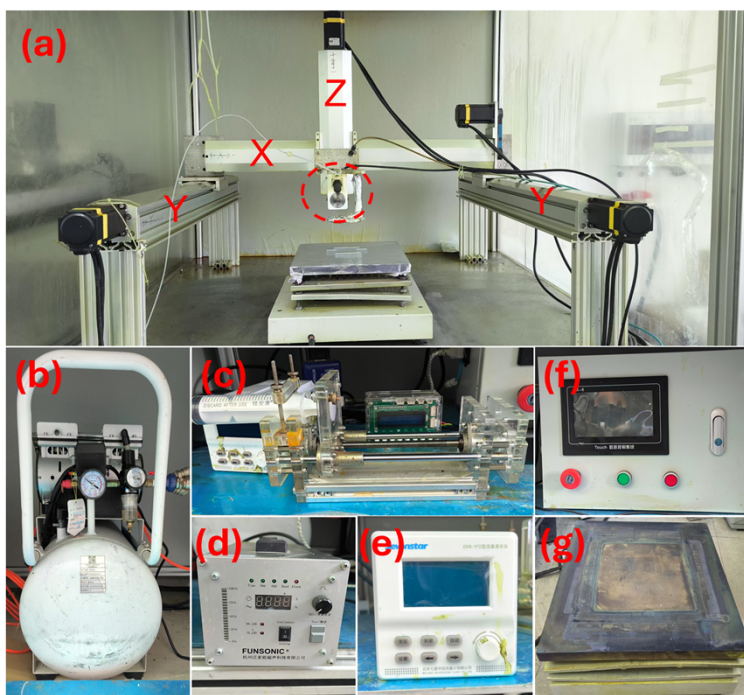


Figure S1. Photographs of our custom-built ultrasonic spray deposition system used for BiOI thin film fabrication.

To meet the experimental requirements, we self-assembled a stable and reliable ultrasonic spray pyrolysis deposition device capable of preparing large-area thin films. As shown in Figure S1(a), which presents the main working area of the spraying device. The ultrasonic atomization nozzle (indicated by the red dotted circle in Figure S1(a)) is fixed on the Z-axis of the three-dimensional sliding module. Directly beneath it is a copper heating stage that provides the requisite temperature for the thermal decomposition reaction. A syringe (c) controls the liquid feed rate of the precursor solution, which is conveyed to the ultrasonic atomization nozzle via a Teflon tube for atomization. An ultrasonic atomization controller (d) regulates the atomization power. The atomized droplets are transported by the carrier gas, generated by an air compressor (b), to the fluorine-doped tin oxide (FTO) substrate on the heating stage for thermal decomposition. The gas flow rate is precisely adjusted by a mass flow meter controller to ensure the stability of the film quality. A numerical control system (f) regulates the operating speed, movement trajectory, and the distance from the nozzle to the substrate of the three-dimensional module. The preparation of large-area films necessitates the use of a large-sized cast copper heating stage (g) providing uniform heating.

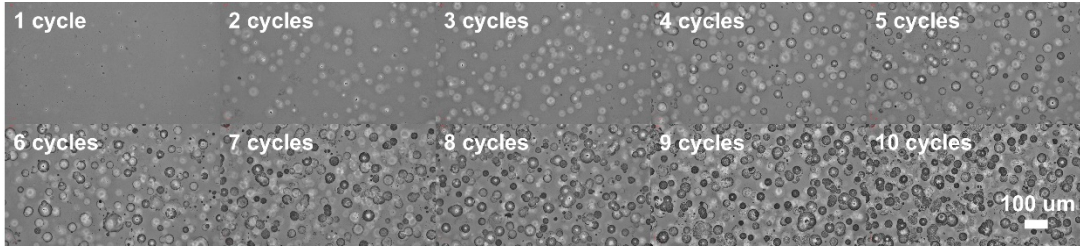


Figure S2. Optical microscope images of continuous spraying for 1-10 cycles at high temperature (350 °C).

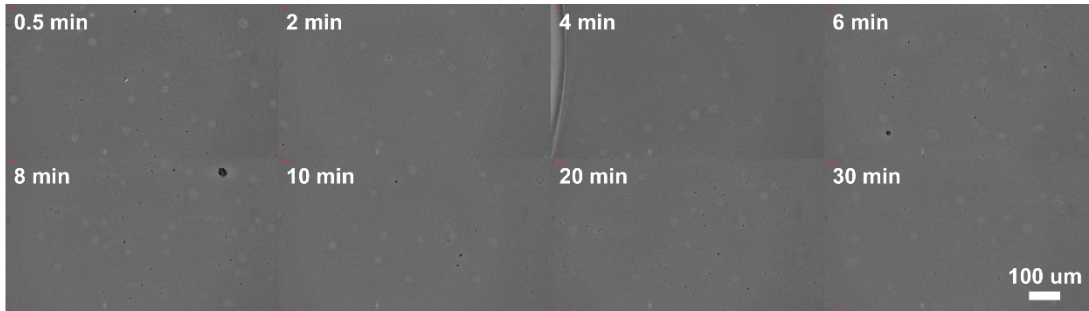


Figure S3. Optical microscope images of FTO sprayed for half a cycle at high temperature, continuously pyrolyzed on a heating stage for 30 minutes, at various time intervals.

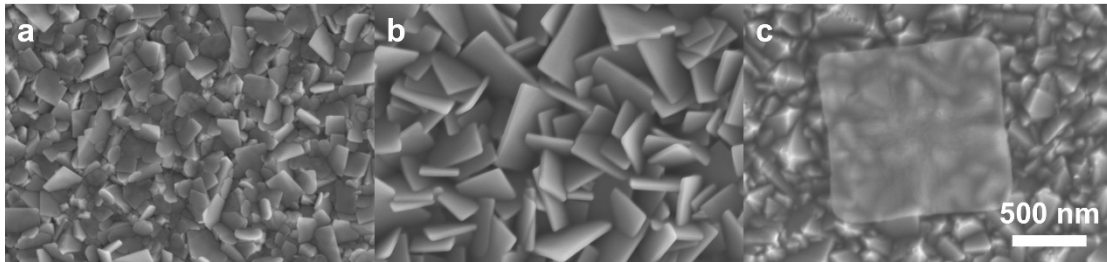


Figure S4. SEM images of the original sample after being sprayed with 10 cycles of different precursor solutions. (a) Original sample. (b) Precursor solution with normal concentration and ratio. (c) Precursor solution without bismuth nitrate pentahydrate.

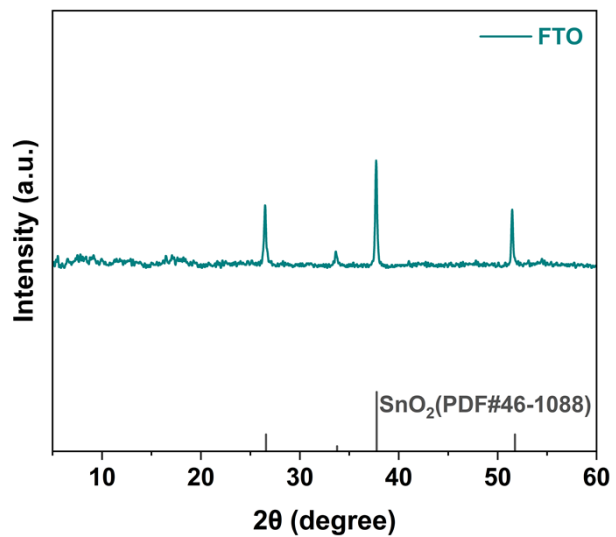


Figure S5. XRD pattern of the FTO substrate.

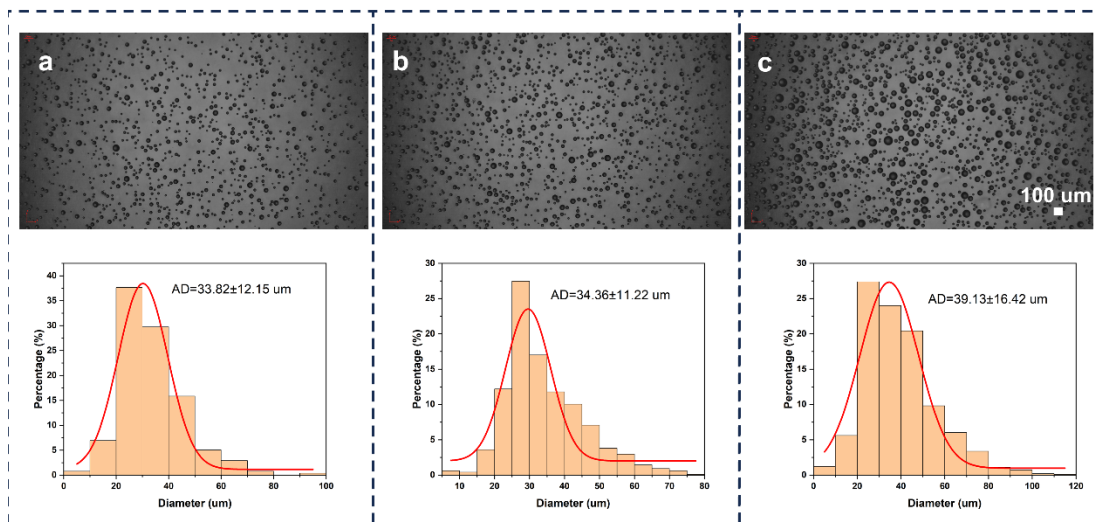


Figure S6. Optical microscope images and statistical sizes of droplet distribution at different liquid feed rates. (a) 30 ml h⁻¹. (b) 60 ml h⁻¹. (c) 120 ml h⁻¹.

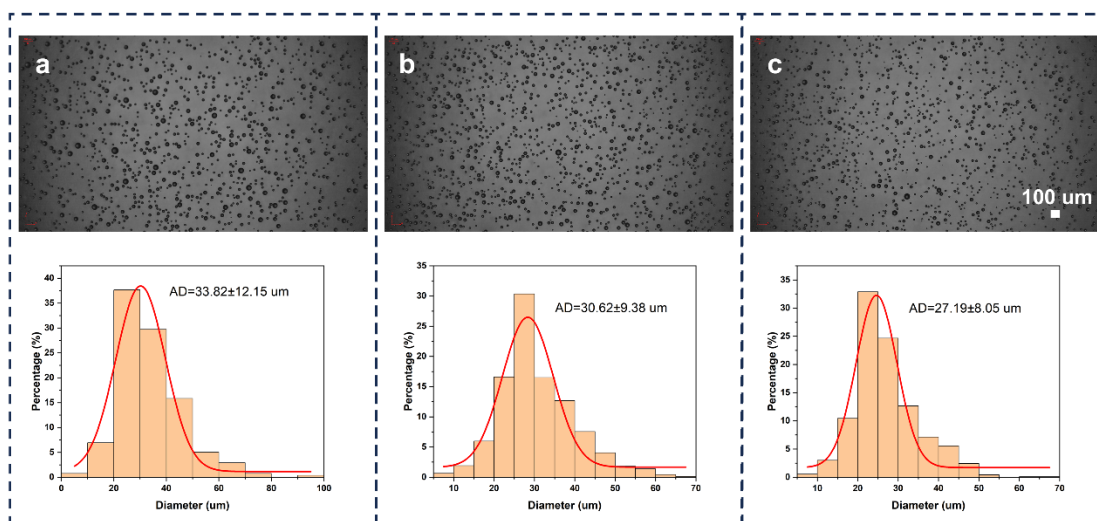


Figure S7. Optical microscope images and statistical sizes of droplet distribution at different gas flow rates. (a) 6 L min^{-1} . (b) 10 L min^{-1} . (c) 14 L min^{-1} .

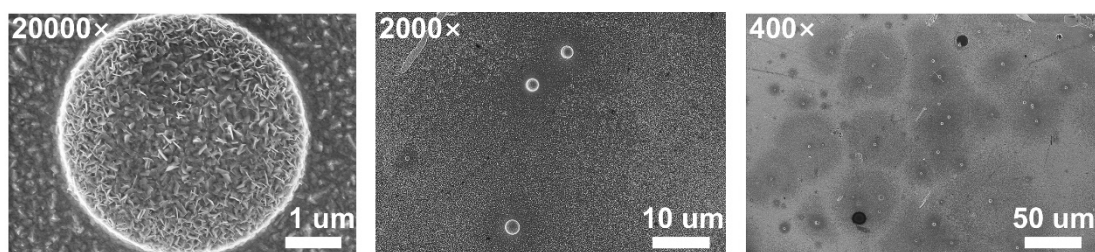


Figure S8. SEM images of BiOI nanoflakes from droplets produced by a high-frequency atomizer at low temperature.

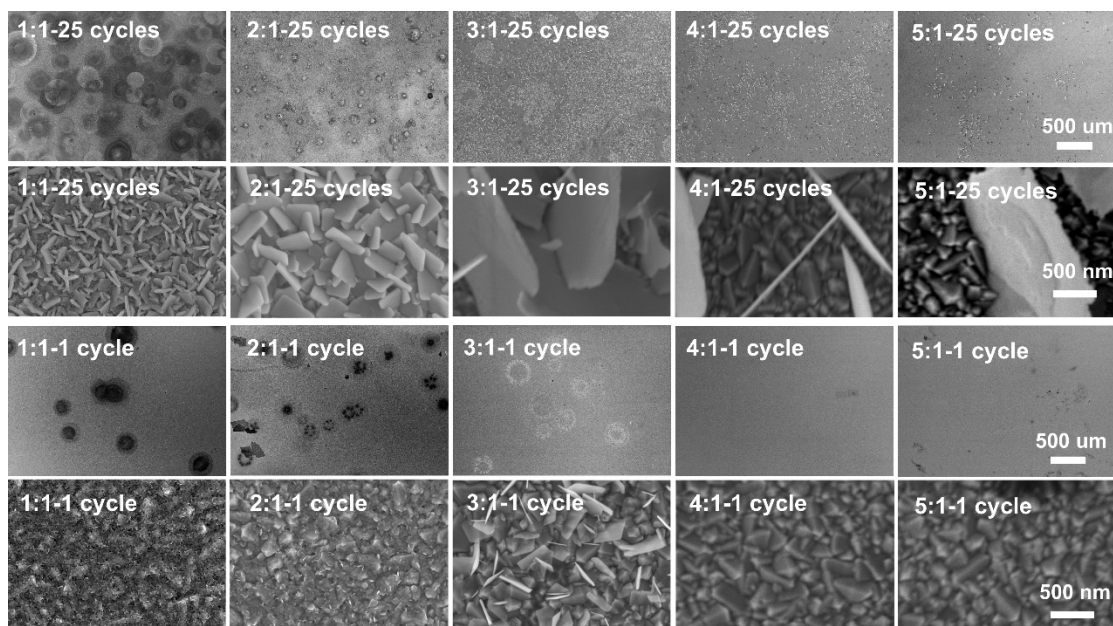


Figure S9. SEM images of different ratio (I: Bi) BiOI after 1 cycle and 25 cycles.

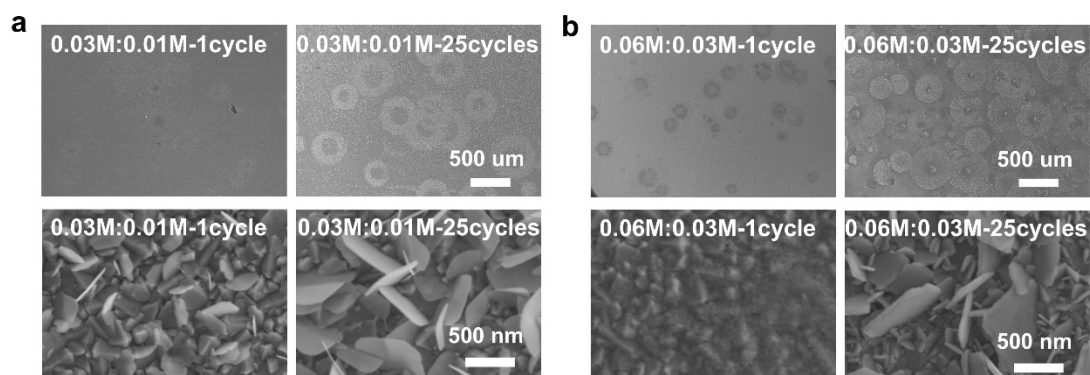


Figure S10. (a) SEM images at low concentration with I: Bi = 3:1. (b) SEM images at high concentration with I: Bi = 2:1.

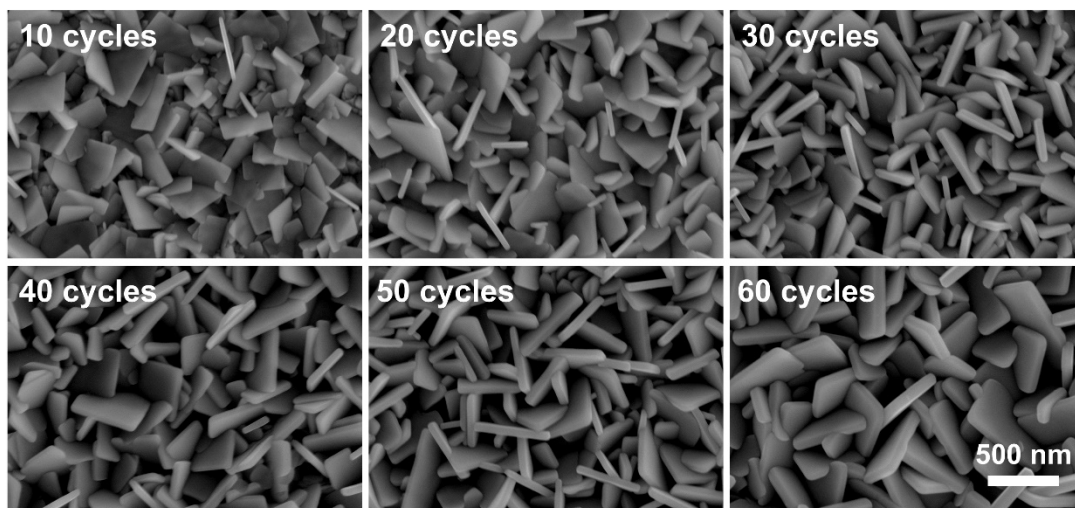


Figure S11. SEM images showing the variation in BiOI nanoflake thickness with the number of spraying cycles.

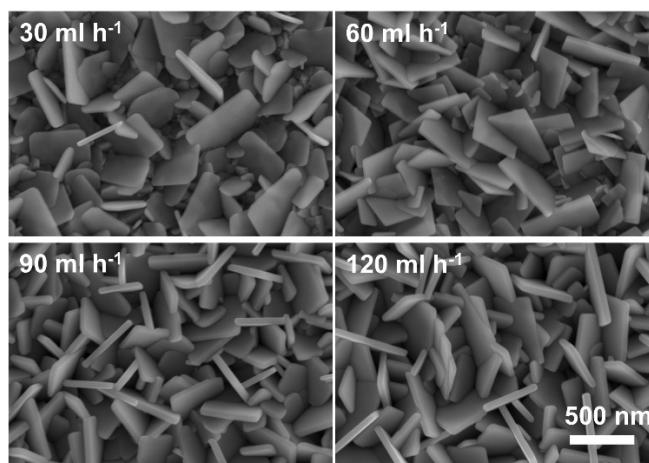


Figure S12. SEM images showing the variation in BiOI nanoflake thickness with changing liquid feed rates.

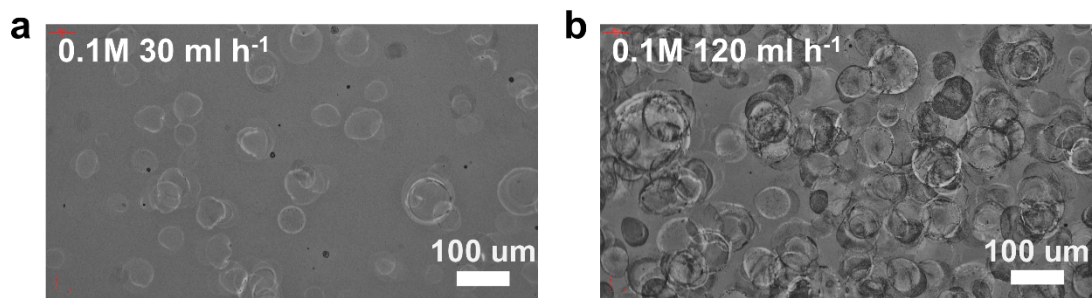


Figure S13. Optical microscope images of droplet behavior at high concentration without Triton. (a) 0.1 mol L⁻¹ - 30 ml h⁻¹. (b) 0.1 mol L⁻¹ - 120 ml h⁻¹.

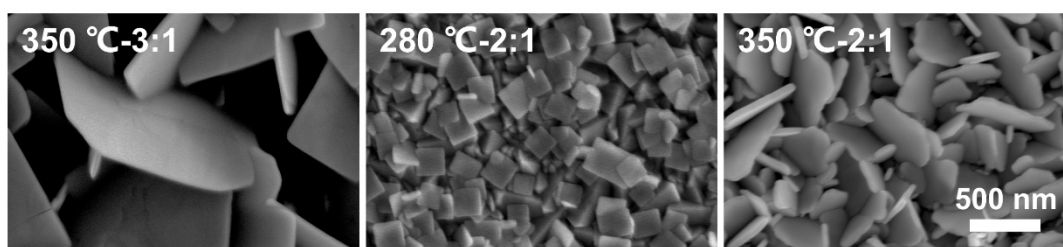


Figure S14. SEM images of BiOI samples with typical morphology.

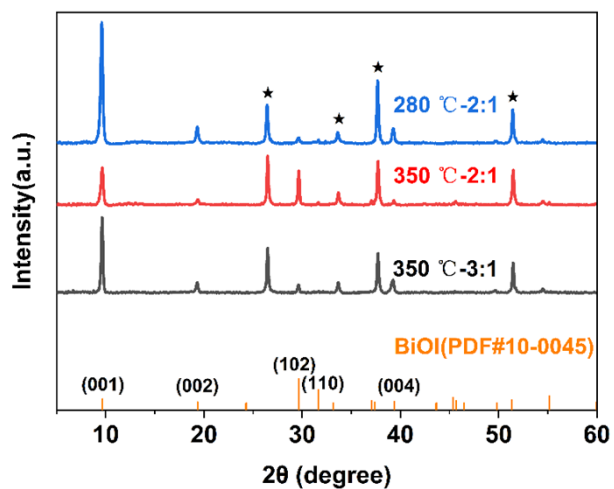


Figure S15. XRD patterns of BiOI samples with typical morphology.

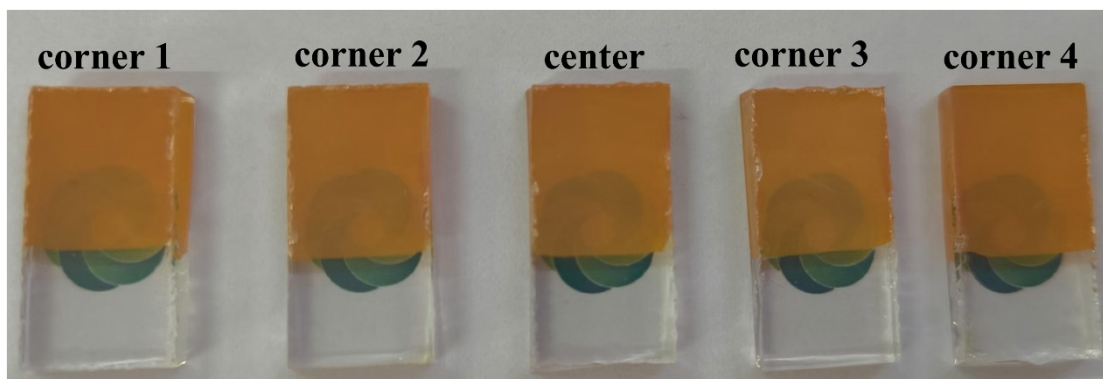


Figure S16. Photographs comparing transmittance in five different regions of large-sized BiOI.

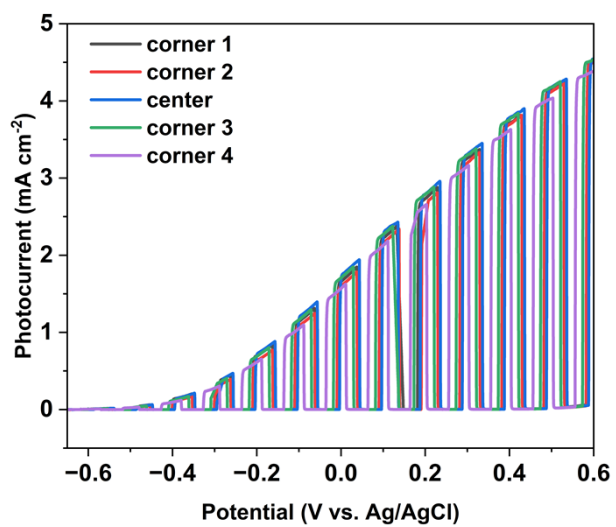


Figure S17. Current-potential curves of five different regions of large-sized BiOI.

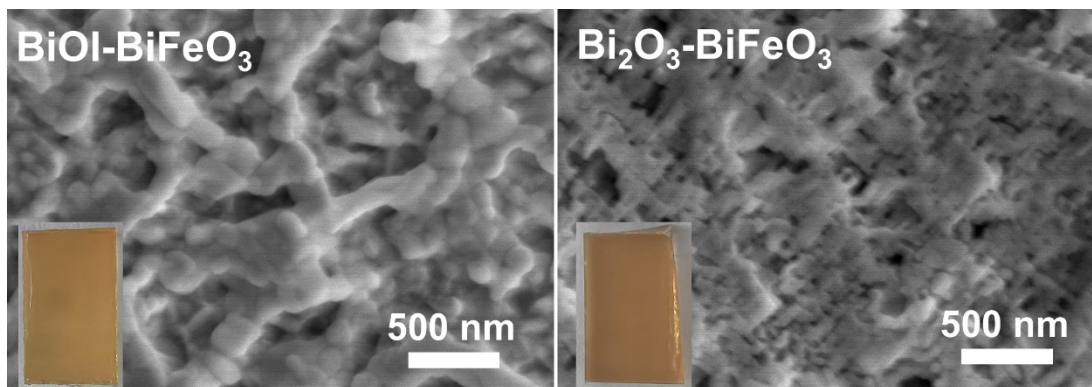


Figure S18. SEM images of converted BiFeO_3 , with inset showing a photograph of the sample.

Table S1. Sizes of BiOI films prepared by different methods as reported

Fabrication method	Film size	Applications	Ref.
spin coating	0.1 cm ²	Solar cell	1
chemical vapor transport	2.54×2.54 cm ²	Solar cell	2
Mist-CVD and Aerosol assisted CVD	1×1 cm ²	photoelectrocatalysis	3
Mist CVD	1.02 × 10 ⁻⁴ cm ²	photodetector	4
Spray pyrolysis deposition	0.21 cm ²	photoelectrocatalysis	5
CVD	0.25 cm ²	photoelectrocatalysis	6
Electrochemical deposition	0.8 × 2.5 cm ²	photocatalysis	7
Solvothermal	4 × 7.5 cm ²	photocatalysis	8
Spray pyrolysis deposition	3.14 cm ²	electrocatalysis	9
Spray pyrolysis deposition	1.2 × 2.5 cm ²	photocatalysis	10
SILAR method	2.6 × 3.8 cm ²	photocatalysis	11
Spray pyrolysis deposition	25 × 25 cm ²	photoelectrocatalysis	This work

REFERENCES

- (1) Feeney, T.; Aygur, G.; Nguyen, T.; Farooq, S.; Mendes, J.; Tuohey, H.; Gómez, D. E.; Della Gaspera, E.; van Embden, J. Solution Processed Bismuth Oxyiodide (BiOI) Thin Films and Solar Cells. *Nanotechnology* 2023, 34 (30), 305404.
- (2) Hoye, R. L. Z.; Lee, L. C.; Kurchin, R. C.; Huq, T. N.; Zhang, K. H. L.; Sponseller, M.; Nienhaus, L.; Brandt, R. E.; Jean, J.; Polizzotti, J. A.; Kursumović, A.; Bawendi, M. G.; Bulović, V.; Stevanović, V.; Buonassisi, T.; MacManus-Driscoll, J. L. Strongly Enhanced Photovoltaic Performance and Defect Physics of Air-Stable Bismuth Oxyiodide (BiOI). *Adv. Mater.* 2017, 29 (36), 1702176.
- (3) Bhachu, D. S.; Moniz, S. J. A.; Sathasivam, S.; Scanlon, D. O.; Walsh, A.; Bawaked, S. M.; Mokhtar, M.; Obaid, A. Y.; Parkin, I. P.; Tang, J.; Carmalt, C. J. Bismuth Oxyhalides: Synthesis, Structure and Photoelectrochemical Activity. *Chem. Sci.* 2016, 7 (8), 4832–4841.
- (4) Sun, Z.; Wang, Y.; Mei, B. Highly Sensitive UV Photodetector Based on Solution-Processed Bismuth Oxyiodide Epitaxial Thin Films. *J. Mater. Chem. C* 2023, 11 (11), 3805–3811.
- (5) Hahn, N. T.; Hoang, S.; Self, J. L.; Mullins, C. B. Spray Pyrolysis Deposition and Photoelectrochemical Properties of N-Type BiOI Nanoplatelet Thin Films. *ACS Nano* 2012, 6 (9), 7712–7722.

- (6) Andrei, V.; Jagt, R. A.; Rahaman, M.; Lari, L.; Lazarov, V. K.; MacManus-Driscoll, J. L.; Hoye, R. L. Z.; Reisner, E. Long-Term Solar Water and CO₂ Splitting with Photoelectrochemical BiOI–BiVO₄ Tandems. *Nat. Mater.* 2022, 21 (8), 864–868.
- (7) Yao, S.; Lai, M.; Yang, J.; Yong, H.; Huang, J.; Wang, X.; Ma, Y. Synthesis and Photocatalytic Properties of Electrodeposited Bismuth Oxyiodide on Rutile/Anatase TiO₂ Heterostructure. *Mater. Res. Express* 2019, 6 (5), 055905.
- (8) Wang, Y.; Long, Y.; Zhang, D. Facile in Situ Growth of High Strong BiOI Network Films on Metal Wire Meshes with Photocatalytic Activity. *ACS Sustainable Chem. Eng.* 2017, 5 (3), 2454–2462.
- (9) Meesombad, K.; Srisawad, K.; Khemthong, P.; Butburee, T.; Sukpattanacharoen, C.; Faungnawakij, K.; Chakthranont, P. Single-Step Fabrication of BiOI Nanoplates as Gas Diffusion Electrodes for CO₂ Electroreduction to Formate: Effects of Spray Pyrolysis Temperature on Activity and Flooding Propensity. *ACS Appl. Nano Mater.* 2024, 7 (17), 20046–20057.
- (10) Arana-Trenado, J. A.; Jayaraman, V. K.; Bizarro, M. Synthesis of (001) Oriented BiOI Thin Films by a Dual-Port Ultrasonic Spray Pyrolysis System. *Mater. Lett.* 2020, 269, 127655.
- (11) Durán-Álvarez, J. C.; Vargas, B.; Mejía, D.; Cortés-Lagunes, S.; Serrano-Lázaro, A.; Ovalle-Encinia, O.; Zanella, R.; Rodríguez, C. A. Synthesis of Highly Crystalline BiOI

Thin Films for the Photocatalytic Removal of Antibiotics in Tap Water and Secondary Effluents: Assessing the Potential Hazard of Treated Water. *J. Environ. Chem. Eng.* 2024, 12 (6), 114590.